Organic & Biomolecular Chemistry

Cite this: *Org. Biomol. Chem.*, 2011, **9**, 6004

www.rsc.org/obc

PAPER

Two-photon induced luminescence, singlet oxygen generation, cellular uptake and photocytotoxic properties of amphiphilic Ru(II) polypyridyl–porphyrin conjugates as potential bifunctional photodynamic therapeutic agents†

JingXiang Zhang,[a] Ka-Leung Wong,[a] Wai-Kwok Wong,*[a,d] Nai-Ki Mak,[b] Daniel W. J. Kwong[a] and Hoi-Lam Tam[c]

Received 16th March 2011, Accepted 17th May 2011
DOI: 10.1039/c1ob05415e

Two Ru(II) polypyridyl-porphyrin and Zn(II) porphyrin conjugates (**Ru-L** and **Ru-Zn-L**) have been synthesized and their photophysical properties studied. The two conjugates, which contained a hydrophobic tetraphenylporphyrin **L** conjugated *via* an acetylide linker at its β-position with a hydrophilic Ru(II) polypyridyl complex, showed high singlet oxygen quantum yields (>70%) and substantial two-photon absorption cross-sections (~500 GM). **Ru-L** gave strong emissions at ~660 and ~733 nm through linear or two-photon excitation. Solvatochromism was observed in the fluorescence spectra of **Ru-L** and **Ru-Zn-L**, where in less polar solvents (*i.e.*, toluene and dichloromethane) their fluorescence emissions became slightly blue-shifted with a 3-fold reduction in intensity relative to those observed in polar solvents (*i.e.*, acetonitrile and methanol). Cell-based studies of these complex conjugates were conducted using human nasopharyngeal carcinoma HK-1 and cervical carcinoma HeLa cells on which **Ru-L** showed rapid cellular uptake, low dark-cytotoxicity, and high photo-cytotoxicity. Furthermore, **Ru-L** can be excited and emits in the "biological window" *in vitro*, making it a potential potent new generation photodynamic therapeutic agent capable of singlet oxygen generation and *in vitro* near-infrared emission.

A. Introduction

The generation of cytotoxic singlet oxygen ($^1O_2$) *in situ* that causes tissue and cellular damage is the basic underlying mechanism of photodynamic therapy (PDT). Thus, PDT requires three major components – molecular oxygen, photosensitizer and appropriate light. Upon photo-irradiation (mostly with linear excitation in the UV-visible region), the photosensitizer is excited to a higher-energy singlet state, where it may undergo intersystem crossing to its lower-energy excited triplet state or returns to its ground state *via* fluorescence emission. In the former scenario, the photosensitizer may react with the molecular oxygen *via* its excited triplet state to generate $^1O_2$.[1]

Photodynamic therapy based on two-photon absorption (TPA-PDT) has attracted great interest recently due to its less-invasive excitation properties.[2] However, porphyrin-based photosensitizers, a popular type of single-photon-activated photosensitizer showing preferential localization at tumors, exhibited low two-photon absorption cross-section σ_2 (<20 GM) and were therefore not considered as prime candidates for TPA-PDT.[3] Thus, a search for novel porphyrin-based photosensitizers with large σ_2 in the near infra-red (NIR) region is going on fervently with attempts to enhance σ_2 *via* (i) extending the π-electron conjugation length[4] and (ii) introduction of intramolecular charge transfer moiety.[5]

However, measurements of $^1O_2$ generation *via* two-photon excitation of porphyrin derivatives showed that large intramolecular charge transfer in the chromophore, which enhances σ_2, can reduce its $^1O_2$ yield.[6] An alternate approach to improve the σ_2 is to link the porphyrin-based photosensitizer to a two-photon absorbing dye where energy can be channeled to the photosensitizer by Förster Resonance Energy Transfer (FRET).[7] By using excitation wavelengths more transparent to the human body (750 nm–1 μm), two-photon sensitization for producing $^1O_2$ became possible. Although certain aforementioned strategies for devising porphyrin-based TPA-PDT photosensitizers have been reported, few have been evaluated *in vitro*. Recently, precision closure of blood vessels through TPA-PDT *in vivo* using porphyrin dimers with large σ_2 has been demonstrated.[8]

[a]*Department of Chemistry, Hong Kong Baptist University, Kowloon Tong, Hong Kong SAR, P. R. China. E-mail: wkwong@hkbu.edu.hk, klwong@hkbu.edu.hk; Fax: +852-3411-5862; Tel: +852-34117011; Tel: +852-34112370*
[b]*Department of Biology, Hong Kong Baptist University, Kowloon Tong, Hong Kong SAR, P. R. China*
[c]*Department of Physics, Hong Kong Baptist University, Kowloon Tong, Hong Kong SAR, P. R. China*
[d]*Centre for Advanced Luminescence Materials, Hong Kong Baptist, University, Kowloon Tong, Hong Kong SAR, P. R. China*

† Electronic supplementary information (ESI) available: ^1H NMR spectra of compounds **Ru-L** and **Ru-Zn-L**, excitation and emission spectra of **L**,**Ru-L** and **Ru-Zn-L**. See DOI: 10.1039/c1ob05415e

The uptake of photosensitizers by tumor cells is a crucial factor in determining tumor imaging and treatment efficacy. In general, cellular uptake depends largely on the hydrophobic and hydrophilic balance of the photosensitizer and it varies in different cell lines. Greater hydrophobicity, which imparts higher cell membrane permeability and therefore higher cellular uptake, will lower the $^1O_2$ yield due to self-aggregation of the photosensitizer. Amphiphilic photosensitizers are pharmacokinetically favorable for rapid systemic clearance and tumor uptake,[9] which is believed to be related to their efficient binding to low-density lipoprotein in the transport of porphyrins to tumor tissues.[10] In addition, controlled intracellular localization of porphyrins, which showed preferential accumulation in solid tumors, in different membrane-limited organelles has been achieved *via* different peripheral charged groups, affording highly selective PDT activity with reduced systemic toxicity.[11] An enhancement in cellular uptake has been demonstrated in Ru(II)-polypyridyl complexes through adjusting the parity between their hydrophilicity and hydrophobicity.[12] Recently, amphiphilic donor–acceptor *meso*-ethynyl porphyrins with a polar pyridinium acceptor head group and a hydrophobic dialkyl-aniline donor, which showed strong second-order nonlinear optical (NLO) activity and high affinities for biological membranes, have emerged to be a new kind of bio-imaging probe *via* second harmonic generation (SHG).[13]

Herein, we report the design and synthesis of two Ru(II)-polypyridyl appended porphyrins (**Ru-L** and **Ru-Zn-L**, Fig. 1) which comprise a hydrophobic porphyrin core (**L** or **Zn-L**) and a hydrophilic charge-transfer moiety, Ru(II)-polypyridyl complex, linked together *via* an acetylide bridge. The relative stabilities, singlet oxygen quantum yields, solvatochromic properties, two-photon induced photophysical and *in vitro* imaging properties of the two porphyrin conjugates (**Ru-L** and **Ru-Zn-L**) are compared, together with their cellular uptake, photo- and dark cytotoxicities in order to assess their potential development as two-photon (NIR) induced imaging and PDT agents. The rationale behind choosing Zn(II) over other metal ions in our design stems from previous observations that Zn(II)-tetraphenylporphyrin exhibits significantly higher triplet state and singlet oxygen quantum yields relative to those of the other metalated and free base tetraphenylporphyrins,[14] thus making **Ru-Zn-L** a potentially better PDT agent.

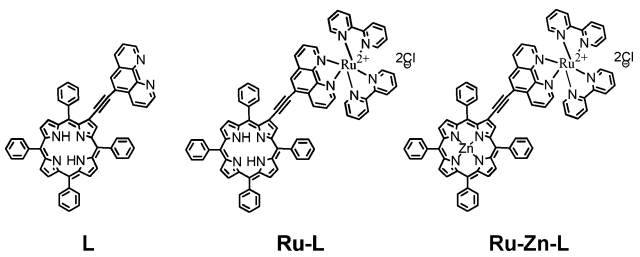

Fig. 1 The molecular structures of porphyrin-based compounds **L**, **Ru-L** and **Ru-Zn-L**.

B. Experimental

All chemicals were of reagent-grade, purchased from Sigma–Aldrich and used without further purification. *cis*-Ru(bpy)$_2$Cl$_2$,[15] 5,6-diamino-1,10-phenanthroline[16] and H$_2$-β-bromotetraphenylporphyrin[17] were synthesized according to literature procedures. All analytical-grade solvents were dried by standard procedures, distilled and deaerated before use. NMR spectra were recorded on a Bruker Ultrashield 400 Plus NMR spectrometer. The ^{1}H NMR chemical shifts were referenced to tetramethylsilane, TMS (δ = 0.00). Mass spectra, reported as m/z, were obtained either on a Bruker Autoflex MALDI-TOF mass spectrometer or a Finnigan TSQ 710 (FAB-MS) mass spectrometer.

Synthesis of ethynyl-1,10-phenanthroline

5-Bromo-1,10-phenanthroline (1.000 g, 3.9 mmol), Pd(PPh$_3$)$_4$ (0.450 g, 0.39 mmol), CuI (0.083 g, 0.43 mmol) and (trimethylsilyl)acetylene (0.590 g, or 0.85 mL, 6.0 mmol) were added to diisopropylamine (10 mL) and stirred. After 24 h, the solvent was distilled off under vacuum and the residue dissolved in methanol (50 mL). Addition of KCN (0.200 g, 3.1 mmol) in water (20 mL) followed by sonication (1 h) resulted in copper decomplexation. It was then chromatographed on silica gel (CH_2Cl_2/methanol = 95/5) to give 0.650 g of a white crystalline product, 5-[2-(trimethysilyl)-1-ethynyl]-1,10-phenanthroline, FAB-MS: 276.3, Calcd, 276. The white solid was treated with K_2CO_3 (0.600 g, 4.35 mmol) in methanol/THF and then chromatographed on silica gel (CH_2Cl_2/CH_3OH = 95/5) to give 0.326 g of a beige crystalline product (41%): ^{1}H NMR ($CDCl_3$) δ 3.63 (s, 1 H), 7.67 (m, 2 H), 8.10 (s, 1 H), 8.24 (d, 1 H, J = 8.2, 1.6 Hz), 8.76 (d, 1 H, J = 8.2, 1.6 Hz), 9.21 (m, 2 H). FAB-MS ([M]$^+$, m/z), Calcd for $C_{14}H_8N_2$ = 204; Found = 204.1.

Synthesis of H$_2$-β-ethynyltetraphenylporphyrin-1,10-phenanthroline (L)

H$_2$-β-Bromotetraphenylporphyrin (200 mg, 0.289 mmol)[17] was dissolved in 20 mL THF. The solution was bubbled with N_2 for 10 min, then Pd(PPh$_3$)$_4$ (80 mg, 0.069 mmol), CuI (10 mg, 0.053 mmol), and a few minutes later, 5-ethynyl-1,10-phenanthroline (164 mg, 0.80 mmol) and 20 mL isopropaldiamine were added. The mixture was stirred overnight at 50 °C. The solvent was removed under vacuum and the residue was chromatographed on silica gel ($CHCl_3$, and then $CHCl_3$: MeOH (v/v) = 100 : 1), the desired product was obtained. Yield: 50.1% (118 mg). ^{1}H NMR ($CDCl_3$) δ –2.65 (s, 2H), 7.49 (m, 2H), 7.73–7.78 (m, 12H), 7.82 (s, 1H), 8.2 (m, 9H), 8.67 (d, 1H, J = 8.27 Hz), 8.76 (m, 3H), 8.83 (d, 1H, J = 8.48 Hz), 8.90 (s, 2H), 9.19–9.24 (m, 3H). MALDI-TOF-MS: [M]$^+$: Calcd for $C_{58}H_{36}N_6$, 817.0; Found for [M + H]$^+$, 818.2; Ana. Calc. for $C_{58}H_{36}N_6$: C 85.27, H 4.44, N 10.29%. Found: C 85.24, H 4.47, N 10.24%.

Synthesis of H$_2$-β-ethynyltetraphenylporphyrin-Ru(phen)-(bpy)$_2$Cl$_2$ (Ru-L)

Porphyrin ligand (**L**) (60 mg, 0.073 mmol) and *cis*-Ru(bpy)$_2$Cl$_2$ (113 mg, 0.233 mmol) were dissolved in a mixture of THF (10 mL) and ethanol (30 mL). The solution was bubbled with N_2 for a few minutes, then refluxed for 15 h. After that the solvent was removed under vacuum and the residue was chromatographed on Al_2O_3 eluted with $CHCl_3$, then $CHCl_3$: MeOH (v/v = 15 : 1). Yield: 80% (75.92 mg). ^{1}H NMR (d_6-DMSO) δ –2.78 (s, 2H), 7.36 (m, 1H), 7.45 (m, 2H), 7.54 (m, 1H), 7.63–7.71 (m, 5H), 7.85 (m, 11H), 7.96 (m, 2H), 8.21 (m, 15H), 8.73 (m, 3H), 8.81 (d, 1H, J = 8.87

Hz), 8.91 (m, 8H), 9.18 (s, 1H). MALDI-TOF-MS: $[M]^+$: Calcd for $[C_{78}H_{52}N_{10}Ru]^+$, 1230.3845; Found, 1230.3386; Ana. Calc. for $C_{78}H_{52}N_{10}RuCl_2$: C 71.99, H 4.03, N 10.76%. Found: C 72.19, H 4.13, N 10.84%.

Synthesis of zinc-β-ethynyltetraphenylporphyrin-Ru(phen)-(bpy)$_2$Cl$_2$ (Ru-Zn-L)

Ru-L (40 mg, 0.030 mmol) was reacted with $Zn(CH_3COO)_2{\cdot}2H_2O$ (33 mg, 0.154 mmol, 5 equiv) in methanol (20 mL) at 65 °C for 5 h. The crude product was washed with water and then dried in vacuum. The pure product was obtained by flash chromatography on Al_2O_3. Yield: 98% (41 mg). ^{1}H NMR (d_6-DMSO) δ 7.28 (m, 1H), 7.45 (m, 4H), 7.63 (m, 4H), 7.68 (d, 1H, J = 5.39 Hz), 7.80 (m, 11H), 7.96 (m, 2H), 8.21 (m, 13H), 8.31 (s, 1H), 8.55 (d, 1H, J = 4.70 Hz), 8.71 (d, 1H, J = 4.44 Hz), 8.76 (m, 4H), 8.91 (m, 4H), 8.81(d, 1H, J = 8.48 Hz), 9.17 (s, 1H). MALDI-TOF-MS: $[M]^+$: Calcd for $[C_{78}H_{50}N_{10}RuZn]^+$, 1294.7659; Found, 1294.2573; Ana. Calc. for $C_{78}H_{50}N_{10}RuZnCl_2$: C 68.65, H 3.69, N 10.26%. Found: C 69.00, H 3.73, N 10.64%.

Linear photophysical measurement

UV-Visible absorption spectra (200 to 1100 nm) were recorded by a HP UV-8453 spectrophotometer. Single-photon luminescence and lifetime spectra were recorded on an Edinburgh Instrument FLS920 Combined Fluorescence Lifetime and Steady State spectrophotometer equipped with a single photon counting photomultiplier in Peltier-cooled housing (185 nm to 850 nm). The spectra were corrected for detector response and stray background light phosphorescence. The quantum yields of the sample solutions were measured by demountable 142 mm (inner) diameter barium sulphide coated integrating sphere supplied with two access ports. The $^1O_2$ quantum yield (Φ_Δ) was measured in terms of its phosphorescence emission intensity at 1270 nm using an InGaAs detector on the PTI QM4 luminescence spectrometer. The $^1O_2$ quantum yields of the conjugates **Ru-L** and **Ru-Zn-L** were determined in chloroform relative to the reference compound *meso*-tetraphenylporphyrin H_2TPP (Φ_Δ = 0.55 ± 0.11) using eqn (1), where Φ_Δ is the singlet oxygen quantum yield, G is the integrated area under the $^1O_2$ emission spectrum and A is the absorbance at the excitation wavelength. Superscripts and subscripts of REF and S correspond to the reference and sample, respectively. In all cases, the $^1O_2$ emission spectra were measured by excitation at 430 nm with the absorbance set at less than 0.05 in order to minimize re-absorption of the emitted light.[17]

$$\Phi_\Delta^S = \Phi_\Delta^{REF} \times \left(\frac{n_S}{n_{REF}}\right)^2 \frac{G_\Delta^S}{G_\Delta^{REF}} \times \frac{A_{REF}}{A_S} \quad (1)$$

Two-photon absorption measurements

Two-photon absorption spectra were measured at 800 nm by the open-aperture Z-scan method using 100 fs laser pulses with a peak power of 276 GW cm^{-2} from an optical parametric amplifier operating at a 1 kHz repetition rate generated from a Ti:sapphire regenerative amplifier system. The laser beam was split into two parts by a beam splitter. One was monitored by a photodiode (D_1) as the incident intensity,[18] and the other beam was detected by the photodiode (D_2) as the transmitted intensity. After passing through a lens with f = 20 cm, the laser-beam was focused and passed through a quartz cell. The position of the sample cell, z, was moved along the laser-beam direction (z-axis) by a computer-controlled translatable table so that the local power density within the sample cell could be changed under the constant incident intensity laser power level. Finally, the transmitted intensity from the sample cell was detected by the photodiode D_2 interfaced to a computer for signal acquisition and averaging. Each transmitted intensity data represent an average of over 100 measurements. Assuming a Gaussian beam profile, the nonlinear absorption coefficient β can be obtained by curve fitting to the observed open-aperture traces, $T(z)$, with eqn(2).[19]

$$T(z) = 1 - \frac{\beta I_0 (1 - e^{-\alpha_0 l})}{2a_0 \left(1 + (z/z_0)\right)^2} \quad (2)$$

where α_0 is the linear absorption coefficient, l is the sample length (1 mm quartz cell) and z_0 is the diffraction length of the incident beam. After obtaining the nonlinear absorption coefficient β, the TPA cross-section σ_2 of the sample molecule (in units of GM, where 1 GM = 10^{-50} cm^4 s photon^{-1}) can be calculated using eqn(3).[20]

$$\sigma_2 = \frac{1000 \beta h \nu}{N_A d} \quad (3)$$

where N_A is the Avogadro constant, d is the concentration of the sample compound in solution, h is the Planck constant, and ν is the frequency of the incident laser beam. The σ_2 reported was the mean value of four independent measurements.

Measurement of dark- and photo-cytotoxicity

Human nasopharyngeal carcinoma HK-1 cells (1×10^4/well in wells of 96-well flat bottom tissue culture plates) were incubated with 2 μM of **Ru-L** and **Ru-Zn-L** in culture medium containing 0.25% DMSO for 24 h in dark. The cells were then replenished with fresh medium and incubated for another 24 h in dark. The cells were washed with phosphate-buffered saline (PBS). Cell viability was then assessed by 3-(4,5-dimethylthiazol-2-yl)-2,5-diphenyl-tetrazolium bromide (MTT) reduction assay. Optical density (OD) of dissolved formazan crystal was measured using a 96-well plate reader (Tecan Infinit F200) at 570 and 690 nm. The percentage of cytotoxicity was calculated using eqn(4):

$$\text{Cytotoxicity (\%)} = \frac{(OD_{control} - OD_{blank}) - (OD_{treatment} - OD_{blank})}{(OD_{control} - OD_{blank})} \times 100 \quad (4)$$

where $OD = OD_{570-690\,nm}$. The photocytotoxicity was assessed by a similar protocol. The cells were exposed to yellow light (3 J cm^{-2}) from a 400 W tungsten lamp fitted with heat-isolation filter and 500 nm long-pass filter at an intensity of 4 mW cm^{-12}.

Fluorometric analysis of cellular uptake

HK-1 cells (2×10^5 cell/well) were incubated separately with 2 μM of **Ru-L** and **Ru-Zn-L** in the culture medium in the dark for 24 h.

Afterward, the cells were washed with phosphate buffered saline (PBS) twice and then trypsinized. The cell-suspended solutions were centrifuged and then washed with PBS for several times. The cell-suspended solutions were then diluted to a final cell concentration of 4×10^5 cell mL^{-1} in PBS. Fluorescence spectra (λ_{ex} = 430 nm) of the cell suspensions were measured fluorometrically. The amounts of conjugates taken up by these cells were estimated semi-quantitatively based on the calibration curves obtained by plotting the fluorescence intensities at 630 nm (for **Ru-L**) and at 620 nm (for **Ru-Zn-L**) *versus* the concentrations of the standard solutions of **Ru-L** and **Ru-Zn-L** in PBS.

Linear and two-photon confocal microscopic analysis of the intracellular localization of Ru-L and Ru-Zn-L

Human HK-1 nasopharyngeal carcinoma cells were maintained in RPMI 1640 medium supplemented with 10% FBS (Gibco) and antibiotics (penicillin 50 U mL^{-1}; streptomycin 50 μg mL^{-1}). The cells were incubated at 37 °C in a humidified incubator with 5% CO_2. Human cervical carcinoma (HeLa) cells were maintained in an RMPI 1640 medium supplemented with 10% fetal bovine serum (FBS) and 1% penicillin and streptomycin in 5% CO_2. HK-1 or HeLa cells (5×10^4/well) were seeded onto cover slip in a 35 mm Petri dish for overnight and incubated with **Ru-L** and **Ru-Zn-L** (1 μM) for 24 h. The linear *in vitro* intracellular localization imaging of **Ru-L** and **Ru-Zn-L** were examined using an Olympus FV1000 confocal microscope. A 60× objective was used for image capturing. Images were processed and analyzed using the FV10-ASW software (Olympus). For the two-photon *in vitro* imaging, the cells were imaged in the tissue culture chamber (5% CO_2, 37 °C) using a Leica SP5 (upright configuration) confocal microscope equipped with a femtosecond-pulsed Ti:Sapphire laser (Libra II, Coherent). The excitation beam produced by the femtosecond laser, which was tunable from 680–1050 nm, (λ_{ex} = 800 nm, ~ 8 mW), was focused on the coverslip-adherent cells through a 40× oil immersion objective.

C. Results and discussion

i) Synthesis and characterisation of L, Ru-L and Ru-Zn-L

The synthetic routes for the porphyrin-1,10-phenanthroline ligand (**L**) and the metal complexes (**Ru-L** and **Ru-Zn-L**) are shown in Scheme 1. Ligand L was synthesized by Pd catalyzed cross-coupling of β-bromotetraphenylporphyrin[17] and 5-ethynyl-1,10-phenathroline in good yield. In the coupling reaction, an excess amount of 5-ethynyl-1,10-phenathroline was used in order to suppress the formation of homocoupling products of β-bromo-tetraphenylporphyrin. L was then treated with *cis*-$Ru(bpy)_2Cl_2$ to afford **Ru-L**, which was purified by chromatographic separation on alumina. **Ru-Zn-L** was obtained in high purity by reacting hydrated zinc acetate with purified **Ru-L**. Both complexes, **Ru-L** and **Ru-Zn-L**, were isolated in high yields (> 80%). ^{1}H NMR spectra (d_6-DMSO) of **L**, **Ru-L** and **Ru-Zn-L** are in good agreement with the proposed structures (see Supporting Information). **Ru-L** and **Ru-Zn-L** were also characterized by MALDI-TOF-MS. The correct $\{M + H\}^+$ peaks were observed with **Ru-L** (m/z = 1230.3388) and **Ru-Zn-L** (m/z = 1294.2573), with small amounts of either sodium or potassium adducts observed.

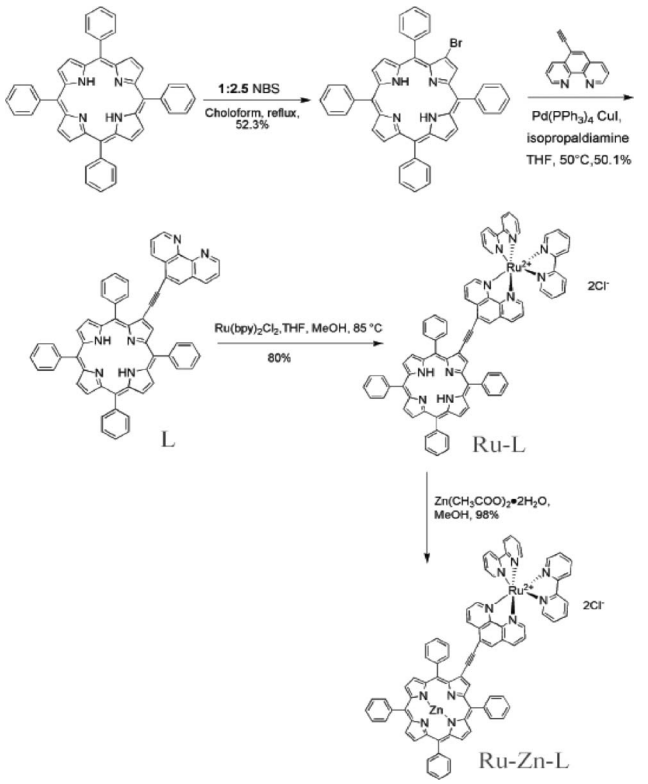

Scheme 1 The synthetic routes to **L**, **Ru-L** and **Ru-Zn-L**.

ii) Linear and two-photon induced photophysical properties

The UV-vis absorption, fluorescence and excitation properties of the porphyrin free base L and its two metal complexes have been examined in DMSO solution (Fig. 2, Fig. 3 and Fig. S5†) and the spectral data are summarized in Table 1 and in the Supporting Information (SI).† Their absorption and fluorescence spectral features are typical of those of porphyrin free bases and metalloporphyrins. The porphyrin free bases **L** and **Ru-L** exhibit a strong Soret band at about 425–429 nm and four weak Q bands between 500–700 nm in their absorption spectra. Upon complexation with Zn(II) ion, the strong Soret band was red-shifted from 429 nm (**Ru-L**) to 439 nm (**Ru-Zn-L**), and the number of Q bands was reduced from four (**Ru-L**; 522, 560, 600 and 657 nm) to three (**Ru-Zn-L**; 571, 612 and 667 nm).[21] Electronic absorption bands located at 290 nm in the two metal complexes are attributed to the $\pi \rightarrow \pi^*$ transition of the bipyridine ligand. The fluorescence spectra obtained by excitation at the Soret bands (430 nm) showed two bands at ~660 and ~733 nm for the porphyrin free bases **L** and **Ru-L**, while those of the metalloporphyrin **Ru-Zn-L** were at ~623 and ~675 nm (Fig. 3). The emission intensities of these two bands diminished more than 30%. These fluorescence changes are typical of complexation of porphyrin free base with Zn(II) ion.[21] The solvent dependence of the photophysical properties of **Ru-L** and **Ru-Zn-L** was examined in organic solvents of different polarities. The absorption (Figure S5) and fluorescence (Fig. 3) intensity of **Ru-L** and **Ru-Zn-L** increases as the solvent polarity increases (toluene < DCM < MeOH < MeCN). The emission lifetime and quantum yields of the two complexes showed a similar trend as the fluorescence intensity, *i.e.*, increased with increasing solvent polarity.[22] The two emission maxima in **Ru-L** (~660 and

Table 1 The photophysical data of **L**, **Ru-L** and **Ru-Zn-L**

Compound	λ_{abs}/nm (log ε)	τ/ns (λ_{em}/nm)	τ/ns (λ_{em}/nm)	Φem/%[a]	Φ_Δ/%[b]	σ/GM[c]
L	425 (5.18), 523 (4.42) 558 (3.91) 598 (3.88) 626 (3.82)	12 (661)	9(622)	11	—	—
Ru-L	287 (4.87), 429 (5.22) 522 (4.32) 560 (3.76) 600(3.62) 657 (3.61)	4(733)	3(663)	5	76	555
Ru-Zn-L	289(4.81), 439 (5.21) 571 (4.21), 612 (4.07) 667 (3.46)	9(675)	7(623)	2	66	485

[a] The emission quantum yields of **L**, **Ru-L** and **Ru-Zn-L** (λ_{em} = 550–800 nm, λ_{ex} = 430 nm). [b] The singlet oxygen quantum yields of **Ru-L** and **Ru-Zn-L** (λ_{ex} = 430 nm). [c] Two-photon absorption cross section (GM = 10^{-50} cm^4 s $photon^{-1}$ $molecule^{-1}$, λ_{ex} = 800 nm).

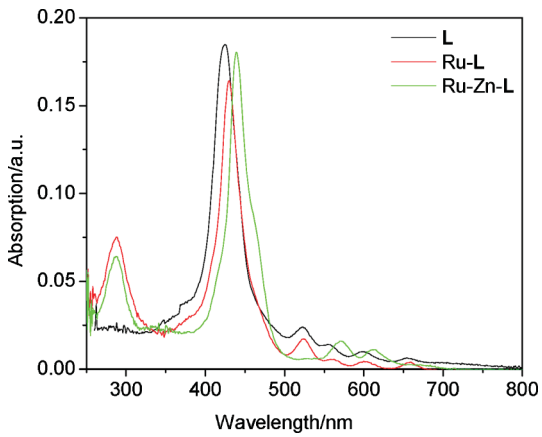

Fig. 2 The UV-vis absorption spectra of **L**, **Ru-L** and **Ru-Zn-L** in DMSO (10^{-6} M).

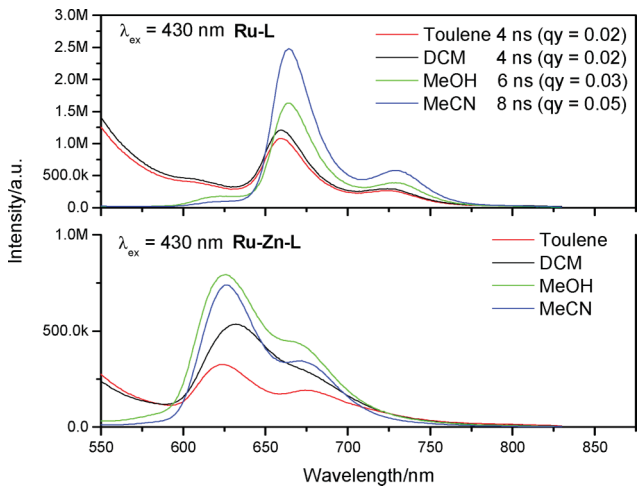

Fig. 3 The emission spectra, lifetimes and quantum yields of **Ru-L** and **Ru-Zn-L** in various solvents (10^{-6} M and λ_{ex} = 430 nm).

~733 nm) and **Ru-Zn-L** (~623 and ~675 nm) do not vary much, only a few nm blue-shifted from methanol to toluene.

In order to evaluate the photosensitizing efficiency of the two conjugates, the $^1O_2$ quantum yields (Φ_Δ) were determined by measuring the NIR phosphorescence intensity of $^1O_2$ (at 1270 nm) produced from these conjugates upon irradiation at 430 nm, using *meso*-tetraphenylporphyrin (H_2TPP) as the reference ($\Phi_\Delta = 0.55 \pm 0.11$), in $CHCl_3$. The $^1O_2$ quantum yield of **Ru-L** ($\Phi_\Delta = 0.76 \pm 0.15$) was significantly higher than that of H_2TPP but was comparable to that of **Ru-Zn-L** ($\Phi_\Delta = 0.66 \pm 0.13$), considering the 20% uncertainty in the measured Φ_Δ of the reference (Table 1 and Figure S7).

To develop these conjugates as imaging probes by multiphoton excitation, the nonlinear photophysical properties of **Ru-L** and **Ru-Zn-L** were examined by ultrafast laser spectroscopy in DMSO. The fluorescence spectra of **Ru-L** and **Ru-Zn-L** upon two-photon excitation at 800 nm (Fig. 4) were found to be similar to those excited at 430 nm (Fig. 3). A power dependence study, which indicates the number of photons involved in the observed emission, confirmed the two-photon excitation (at 800 nm) nature of these emission bands (inset of Fig. 4), where the intensity of the two-photon excited fluorescence (TPEF) showed a linear dependence on the square of the power of the incident laser beam.

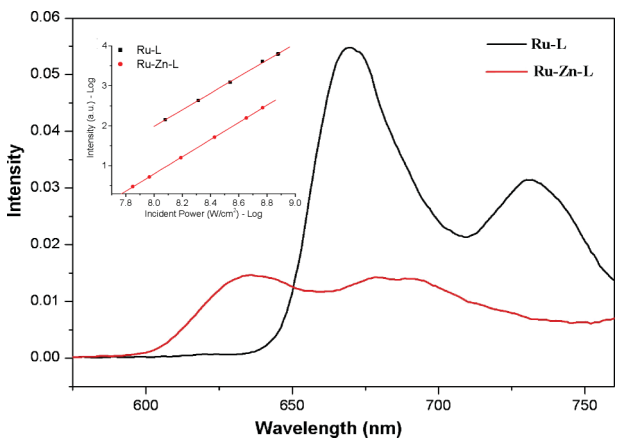

Fig. 4 TPA-induced fluorescence of **Ru-L** and **Ru-Zn-L** (4 mM) excited at 800 nm in DMSO. Inset: The power dependence study of **Ru-L** and **Ru-Zn-L** (λ_{ex} = 800 nm, **Ru-L**: λ_{em} = 740 nm and **Ru-Zn-L**: λ_{em} = 675 nm, slope ~ 2.0).

In general, the two-photon absorption cross-section of a material in solution is indicative of its two-photon absorption strength and hence its potential for two-photon induced *in vitro* imaging.[22] The two-photon absorption cross-sections of **Ru-L** and **Ru-Zn-L**, measured by the Z-scan method,[12] were determined to be 555 and 485 GM, respectively (Fig. 5).

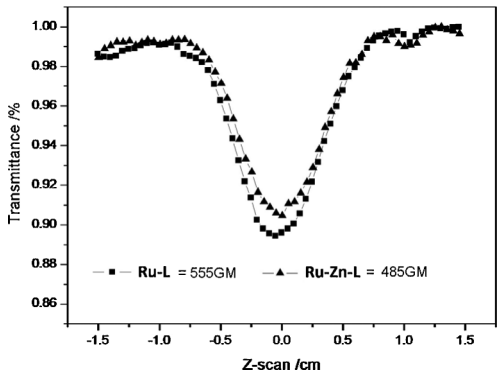

Fig. 5 Open-aperture Z-scan trace of **Ru-L** and **Ru-Zn-L** (4 mM) excited at 800 nm in DMSO. The average power of the laser beam was 0.271 mW. (GM = 10^{-50} cm^4 s).

iii) Cellular uptake, *in vitro* imaging and cytotoxic properties of Ru-L and Ru-Zn-L

The uptake of a photosensitizer by tumor cells is a critical determinant of its treatment efficacy. The cellular uptake of the two conjugates were studied fluorometrically in nasopharyngeal carcinoma HK-1 cells and by multiphoton laser scanning confocal microscopy in human cervical carcinoma HeLa cells. Fig. 6 shows the uptake of **Ru-L** and **Ru-Zn-L** by HK-1 cells based on fluorometric analysis. The results show that the uptake of **Ru-L** was *ca*. 75% higher than that of **Ru-Zn-L**. Similar results were found in the confocal microscopic imaging of the HeLa cells through linear and two-photon excitation. In this experiment, HeLa cells were dosed with equal amounts of **Ru-L** or **Ru-Zn-L** and their fluorescence images were monitored at various time points (after 2, 3 and 4 h) of incubation. Red emission can be observed clearly by visible (λ_{ex} = 432 nm) and NIR excitation (two-photon, λ_{ex} = 800 nm). Strong red emission can be seen on the cell membrane but not inside the cells after two hours of incubation with either **Ru-L** or **Ru-Zn-L** (Fig. 7). After 3 h of incubation, the strong red emission of **Ru-L** was observed in the cytoplasm of HeLa cells, with no obvious organelle localization (Fig. 7b). But for **Ru-Zn-L**, its red emission remained at the cell membrane with no apparent uptake into the HeLa cells. Weak emission from **Ru-Zn-L** was observed in the cytoplasm only after 4 h of incubation (Fig. 7). These observations show that the cellular uptake of **Ru-L** is 40% faster than that of **Ru-Zn-L** in HeLa cells, which is consistent with the results obtained in the HK-1 cells (Fig. 6).

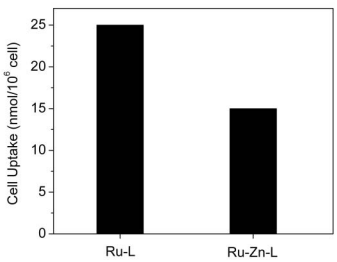

Fig. 6 Fluorometric analysis of the cellular uptake of 2 μM of **Ru-L** and **Ru-Zn-L** by HK-1 cells after 24-hour incubation.

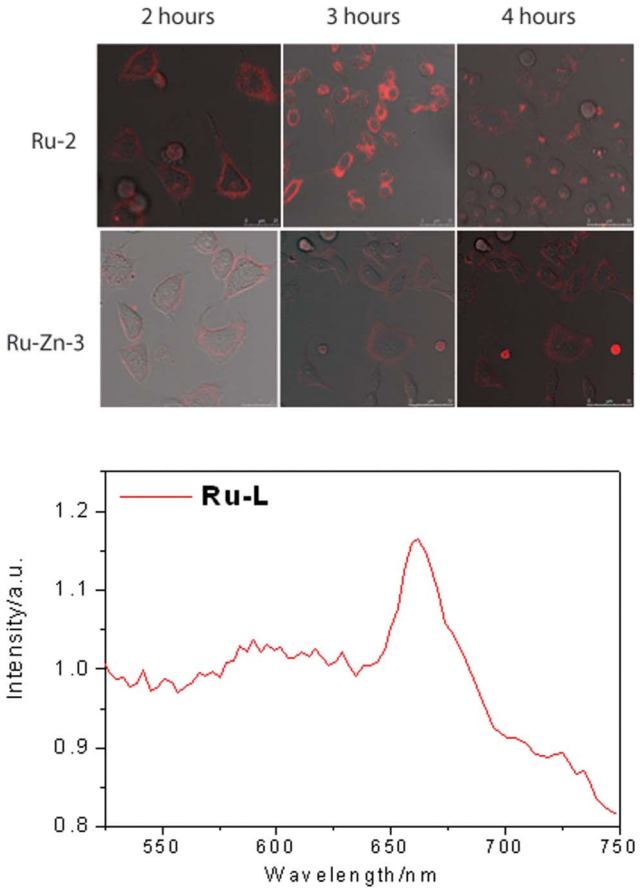

Fig. 7 (a) Confocal microscopic images of **Ru-L** (upper row) and **Ru-Zn-L** (bottom row) in HeLa cells obtained at various time points (2, 3 and 4 h) of incubation with 5 μM of the conjugates (λ_{ex} = 800 nm, λ_{em} = 450–750 nm). (b) *In vitro* emission spectrum of **Ru-L** in HeLa cells obtained after 4 h of incubation by λ scan on a Leica SP5 confocal microscope (resolution ~6 nm, λ_{ex} = 800 nm).

To confirm that the red emission found in the cytoplasm was due to the two-photon induced emission from **Ru-L**, the *in vitro* emission spectrum obtained by λ scan of the confocal microscope (resolution = 6 nm, λ_{ex} = 800 nm) was taken. This emission spectrum (Fig. 7b) resembles very closely the TPA-induced emission spectrum of **Ru-L** obtained under cell-free conditions (Fig. 4), thus confirming the uptake of **Ru-L** into the cytoplasm of the HeLa cells.

Since both **Ru-L** and **Ru-Zn-L** showed strong emission and $^1O_2$ generation with one-photon excitation, these conjugates can potentially qualify as bifunctional tumor-imaging and photodynamic therapeutic agents. To evaluate the therapeutic efficacy of **Ru-L** and **Ru-Zn-L**, their photo-cytotoxicity towards HK-1 cells was measured by MTT reduction assay and compared to their cytotoxicities measured without photo-irradiation. From Fig. 8, it can be seen that **Ru-L** and **Ru-Zn-L** were essentially non-cytotoxic in the absence of light, but were substantial photocytotoxic at 1 μM concentration and under a light dose of 3 J cm^{-2}, where 80% and 50% of the HK-1 cells incubated with **Ru-L** and **Ru-Zn-L**, respectively, were killed.

The efficacy of the photodynamic and fluorescent imaging properties of **Ru-L** and **Ru-Zn-L** under two-photon excitation in HeLa cells were studied as well and the results are shown in

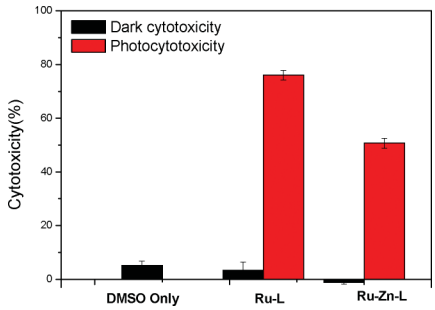

Fig. 8 Dark cytotoxicity (black) and photo-cytotoxicity (red, with 3 J cm^{-2} light dose) of **Ru-L** and **Ru-Zn-L** on HK-1 cells.

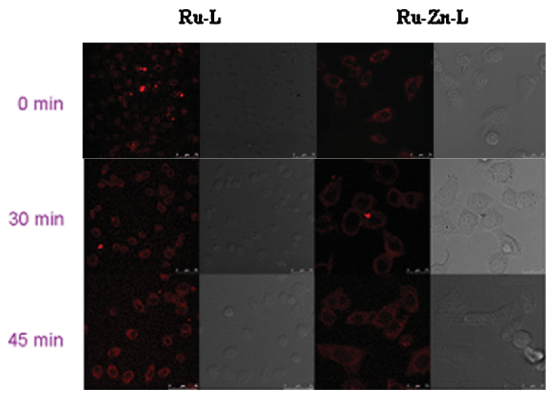

Fig. 9 Confocal microscopic and bright-field images of HeLa cells loaded with **Ru-L** (left) and **Ru-Zn-L** (right). Top row: images observed for **Ru-L** (left) and **Ru-Zn-L** (right) after 3 h of incubation with a snap laser flash (to avoid $^1O_2$ generation) at 800 nm; middle row: images observed after 30 min of laser flashes at 800 nm; bottom row: images observed after 45 min of laser flashes at 800 nm.

Fig. 9. After 3 h of incubation, both **Ru-L** and **Ru-Zn-L** were taken up by the HeLa cells, as revealed by their red emission in the cytoplasm induced by a short 800 nm laser flash (Fig. 9, top row). Under continuous 800 nm laser flashes for 30 min, *ca.* 70% of the cells incubated with **Ru-L** became deformed and lost their morphological integrity, which indicated cell death. However, no significant morphology change was seen in those cells loaded with an identical dose of **Ru-Zn-L** under the same laser excitation conditions at 800 nm.

Conclusions

Two amphiphilic Ru(II) polypyridyl-porphyrin and Zn(II) porphyrin conjugates, **Ru-L** and **Ru-Zn-L**, have been synthesized and their linear and two-photon induced photophysical properties measured. **Ru-L** exhibited emission in the near-infrared region (λ_{em} = 675 nm) by one- and two-photon (λ_{ex} = 800 nm) excitations. It further showed high quantum efficiency and $^1O_2$ quantum yield (*ca.* 76%). The complexation of **Ru-L** with Zn(II) in **Ru-Zn-L** blue-shifted the two emission bands by *ca.* 40 nm and also reduced the quantum efficiency substantially. The reasons for this are not presently understood. From cell-based studies, **Ru-L** showed a faster cell uptake rate and a stronger photo-cytotoxicity than **Ru-Zn-L**. Thus, **Ru-L**, with its high $^1O_2$ quantum yield and strong NIR emission, showed great potential to be a bifunctional tumor-imaging and photodynamic therapeutic agent by two-photon excitation.

Acknowledgements

The work described in this paper was partially supported by grants from the Research Grants Council of the Hong Kong SAR, P.R. China (HKBU 202308 and HKBU 202509) and a grant from the Hong Kong Baptist University (FRG2/08-09/067).

Notes and references

1 B. W. Henderson and T. J. Dougherty, *Photodynamic Therapy: Basic Principles and Clinical Application*, Marcel Dekker, New York, 1992; E. S. Nyman and P. H. Hynninen, *J. Photochem. Photobiol., B*, 2004, **73**, 1; K. Lang, J. Mosinger and D. M. Wagnerova, *Coord. Chem. Rev.*, 2004, **248**, 321; J. Lovell, T. W. B. Liu, J. Chen and G. Zheng, *Chem. Rev.*, 2010, **110**, 2839; J. P. Celli, B. Q. Spring, I. Rizvi, C. L. Evans, K. S. Samkoe, S. Verma, B. W. Pogue and T. Hasan, *Chem. Rev.*, 2010, **110**, 2795.
2 K. Ogawa and Y. Kobuke, *Anti-Cancer Agents Med. Chem.*, 2008, **8**, 629; S. Brown, *Nat. Photonics*, 2008, **2**, 394.
3 A. Karotki, M. Khurana, J. R. Lepock and B. C. Wilson, *Photochem. Photobiol.*, 2006, **82**, 443.
4 Y. Nakamura, S. Y. Jang, T. Tanaka, N. Aratani, J. M. Lim, K. S. Kim, D. Kim and A. Osuka, *Chem.–Eur. J.*, 2008, **14**, 8279; J. Dy, K. Ogawa, K. Kamada, K. Ohta and Y. Kobuke, *Chem. Commun.*, 2008, 3411; J. T. Dy, K. Ogawa, A. Satake, A. Ishizumi and Y. Kobuke, *Chem.–Eur. J.*, 2007, **13**, 3491; M. Drobizhev, Y. Stepanenko, Y. Dzenis, A. Karotki, A. Rebane, P. N. Taylor and H. L. Anderson, *J. Am. Chem. Soc.*, 2004, **126**, 15352; M. Morone, L. Beverina, A. Abbotto, F. Silvestri, E. Collini, C. Ferrante, R. Bozio and G. A. Pagani, *Org. Lett.*, 2006, **8**, 2719.
5 K. S. Kim, S. B. Nok, T. Katsuda, S. Ito, A. Osuka and D. Kim, *Chem. Commun.*, 2007, 2479.
6 P. K. Frederiksen, S. P. Mcllroy, C. B. Nielsen, L. Nikolajsen, E. Skovsen, M. Jorgensen, K. V. Mikkelsen and P. R. Ogilby, *J. Am. Chem. Soc.*, 2005, **127**, 255.
7 M. A. Oar, W. R. Dichtel, J. M. Serin, J. M. J. Fréchet, J. E. Rogers, J. E. Slagle, P. A. Fleitz, L.-S. Tan, T. Y. Ohulchanskyy and P. N. Prasad, *Chem. Mater.*, 2006, **18**, 3682.
8 S. Kim, T. Y. Ohulchanskyy, H. E. Pudaver, R. K. Pandey and P. N. Prasad, *J. Am. Chem. Soc.*, 2007, **129**, 2669.
9 R. Bonnett, *Rev. Contemp. Pharmacother.*, 1999, **10**, 1.
10 D. Kessel, P. Thompson, K. Saatio and K. D. Nantwi, *Photochem. Photobiol.*, 1987, **45**, 787.
11 N. Nishiyama, H. R. Stapert, G.-D. Zhang, D. Takasu, D.-J. Jiang, T. Nagano, T. Aida and K. Kataoka, *Bioconjugate Chem.*, 2003, **14**, 58.
12 C. A. Puckett and J. K. Barton, *Biochemistry*, 2008, **47**, 11711; C. A. Puckett and J. K. Barton, *J. Am. Chem. Soc.*, 2007, **129**, 46; U. Schatzschneider, J. Niesel, I. Ott, R. Gust, H. Alborzinia and S. Wolfl, *ChemMedChem*, 2008, **3**, 1104.
13 J. E. Reeve, H. A. Collins, K. D. Mey, M. M. Kohi, K. J. Thorley, O. Paulsen, K. Clays and H. L. Anderson, *J. Am. Chem. Soc.*, 2009, **131**, 2758.
14 M. Pineiro, A. L. Carvalho, M. M. Pereira, A. M. d'A Rocha Gonsalves, L. G. Arnaut and S. J. Formosinho, *Chem.–Eur. J.*, 1998, **4**, 2299; H. Ke, H. Wang, W.-K. Wong, N.-K. Mak, D. W. J. Kwong, K.-L. Wong and H.-L. Tam, *Chem. Commun.*, 2010, **46**, 6678.
15 B. P. Sullivan, D. J. Salmon and T. J. Meyer, *Inorg. Chem.*, 1978, **17**, 3334.
16 A. Kleineweischede and J. Mattay, *Eur. J. Org. Chem.*, 2006, 947.
17 G.-Y. Gao, J. V. Ruppel, D. B. Allen, Y. Chen and X. P. Zhang, *J. Org. Chem.*, 2007, **72**, 9060.
18 M. Sheik-Bahae, A. A. Said, T.-H. Wei, D. J. Hagan and E. W. Van Stryland, *IEEE J. Quantum Electron.*, 1990, **26**, 760.
19 Y. Li, T. M. Pritchett, J. Huang, M. Ke, P. Shao and W. Sun, *J. Phys. Chem. A*, 2008, **112**, 7200.
20 K. Wang, C.-T. Poon, W.-K. Wong, W.-Y. Wong, C. Y. Choi, D. W. J. Kwong, H. Zhang and Z.-Y. Li, *Eur. J. Inorg. Chem.*, 2009, 922.
21 H.-Z. Yu, J. S. Baskin and A. H. Zewail, *J. Phys. Chem. A*, 2002, **106**, 9845.
22 M. Maiti and R. P. Steer, *Chem. Phys. Lett.*, 2009, **482**, 254.